IJEIT
The International Journal of Engineering and Information Technology
journal homepage:www.ijeit.misuratau.edu.ly
MISURATA UNIVERSITY

Comparative Analysis for Off-Board Vienna Rectifier Electric Vehicle Charger Controlled by VOC and DPC Techniques

Aiman Nouh
Department of Electrical & Electronic Engineering, University of Omar Al-Mukhtar, Al-Bayda, Libya
aiman.nouh@omu.edu.ly

Waled Sulieman Ali
Department of Electrical & Electronic Engineering, University of Omar Al-Mukhtar, Al-Bayda, Libya

Moneer A. Faraj
Department of Electrical & Electronic Engineering, University of Omar Al-Mukhtar, Al-Bayda, Libya

Abstract—**Electric vehicle charging stations are generally composed of AC-to-DC and DC-to-DC converters. Many topologies of converters, used for both on-board and off-board EV chargers, have been proposed by the researchers. The off-board Vienna rectifier EV charger is the focus of our work. This EV charger should be controlled for adjusting the system outputs at desired references. Among several control methods existing in the literature, the voltage-oriented and direct power control techniques are selected to control the Vienna rectifier. The aim of this paper is to present a comparative analysis for an Off-board Vienna rectifier controlled individually by the previous mentioned control techniques in order to charge the battery of an electric vehicle from the national grid. A three constant current values of 60A, 80A, and 100A, are imposed to the EV battery as reference currents using PI controllers. The comparison is based on the waveforms of three-phase grid voltages and currents, battery voltages, state of the charge of the battery, and the elapsed time of simulation. The total harmonic distortion (THD) of one phase of the input current at the case of 100A is measured using the fast Fourier transform tool of Matlab/Simulink software which employed for modeling and performing the simulation. The obtained results reveal that the voltage-oriented control technique is better than the direct power control technique in terms of THD with 1.87% and 5.88% respectively. In terms of simulation time, the direct power control method is much lesser than the voltage-oriented control method with a few hours and up three days respectively.**

Index Terms—**off-board electric vehicle charger, Vienna rectifier, voltage-oriented control, direct power control.**

I. INTRODUCTION

This paper is motivated by the search for the quality of life that electrified transportation offers. Electric Vehicles (EVs), as a promising technology, participate in this improvement of the quality of life where they gradually replace their peer internal combustion engine (ICE) vehicles. These last inject different pollutants into the environment that degrade the air quality leading to health concerns. According to the literature, ICE vehicles are responsible for 29% of greenhouse gas emissions in the US [1], and account for 15% of total fossil fuel consumption [2]. EVs have gained wide acceptance worldwide due to their fuel independency [3][4], zero emissions target from 2030 onwards, and increasing global sales by up to 70% with an annual growth record of 4.6% in 2020 [5]. Despite these merits, the size, weight, storage capacity, and lifespan limitations of rechargeable battery technology as well as its high cost are the major challenges that EVs development faces. To overcome these demerits, researchers, automobile manufacturers, and governments push most of the electric utility industries to upgrade the electric power grids in such a way that they handle the bidirectionality of power flow and the entering/outing of different loads as well as a variety of sources (including conventional and renewables). Based on this upgradability, the concepts of vehicle-to-grid (V2G) and grid-to-vehicle (G2V) can be adopted. On-board and off-board EV chargers are existed with unidirectional and bidirectional. Off-board unidirectional charger is the focus of this research because it permits high power flow, is designed for fast and ultra-fast charging, reduces the volume and weight of EVs, and overcomes the limits of on-board chargers [2][5][6]. The concept of EVs station evolves both AC bus and DC bus. Concepts with AC bus suffer from more conversion stages and high cost and complexity, while structure with DC bus offers more flexibility, isolating grid side, lesser rectifiers, high efficiency, and simple controllability [2][6]. Generally, an EV charging station consists of two conversion stages, firstly the AC-DC rectifier that ensures high efficiency, regulated output DC voltage, simple switching techniques, less total harmonics distortion (THD) using power factor correction (PFC) techniques so improving the power quality, and compensating the reactive power. In the second stage, a DC-DC converter is used to satisfy requirements like high efficiency, less output voltage ripple, high-frequency switching, and a broad variety of output voltage (40-1000 VDC) compatible with different levels of battery voltage standards [2][5-7]. Authors of [2][7] were conducted a comprehensive review search on the converter topologies used for EVs charging stations.

Received 18 Oct , 2023; revised 26 Feb, 2024; accepted 01 Mar 2024.

Available online 22 Mar, 2024.

Several configurations were well-detailed in the literature for the first conversion stage (AC to DC). Among these topologies, the two-level active front end (AFE), three-level neutral point clamped (NPC) AFE, three-level T-type AFE, Vienna rectifier (VR), Swiss rectifier (SR), and matrix converter-based isolated AC/DC converter. They differ from each to the other based on the number of active/passive switches, semiconductor voltage stress, power direction, filter size, power density, and the complexity of the control. Vienna rectifier was adopted in this research for its superior features including the satisfying of grid-side requirement, less number of switches, low THD, neutral connection-free structure, no galvanic isolation, boost type rectifier, small filter size, and moderate control. Despite this, VR has drawbacks like the distortion of grid-side current at the zero-crossing, anti-load sudden ability, and the need for DC-link capacitors [2][7-9]. The second conversion stage (DC to DC) can be classified as non-isolated and isolated converters. Buck converter, interleaved buck converter, three-level NPC buck converter, three-level flying capacitor buck converter, and non-inverting buck-boost converter, all are non-isolated DC-DC converters. While, dual active bridge (DAB), CLLC converter (similar to DAC with series LC resonant at primary and secondary sides), three-level FC-DAB, three-level NPC-DAB, LLC converter, and phase-shifted full-bridge converter, all are isolated DC-DC converters. The conventional buck converter is selected as the DC-DC converter in this research because of the less number of components, the low ripple of its output side current, and the high power density. However, a downside of having large inductors and semiconductor switching loss [2][7].

Several control strategies have been reported in the literature [2][3][7][9] for the AC-to-DC conversion stage. Voltage-oriented control (VOC), direct power control (DPC), virtual flux (VF), sliding-mode control (SMC), hysteresis control (HC), fuzzy logic control (FLC), model predictive control, adaptive control, and neural-network control, are all control approaches used for AC-to-DC EV chargers. In the DC-to-DC conversion stage, approaches like the feedback control, PI/PID controller, disturbance-observer, and SMC, can be used. In this paper, firstly, the VOC approach is used to control the VR in order to mitigate the output DC voltage ripple, input current THD, and grid-side power factor [3][8][10]. Secondly, The DPC approach is applied instead of VOC to control VR due to its feature of direct regulation of active and reactive power components [11].

There is a lack in the literature concerning the controlling of VR-EV charger using the DCP technique. The few papers found in the literature were considered a small simulation time (0.2-1.5 S). Generally, they considered a resistive load instead of a battery model. The variation of the state of charge (SoC) and the time needed to reach the full charging were not taken into account [12][13]. In addition, there are no researches that compare VR-VOC and VR-DPC. In this context, the research gap can be identified firstly by modeling a VR-EV charger, then integrating VR-VOC and VR-DPC considering a battery model and long simulation time enough to reach the full charging, and finally comparing the obtained results. Our adopted methodology in order to fill this research gap is depicted in Fig.1 as a flowchart.

The objectives of this research are the following:

- To model and simulate, using Matlab/Simulink software, an off-board Vienna EV charger controlled once by the VOC method and another by the DPC method.

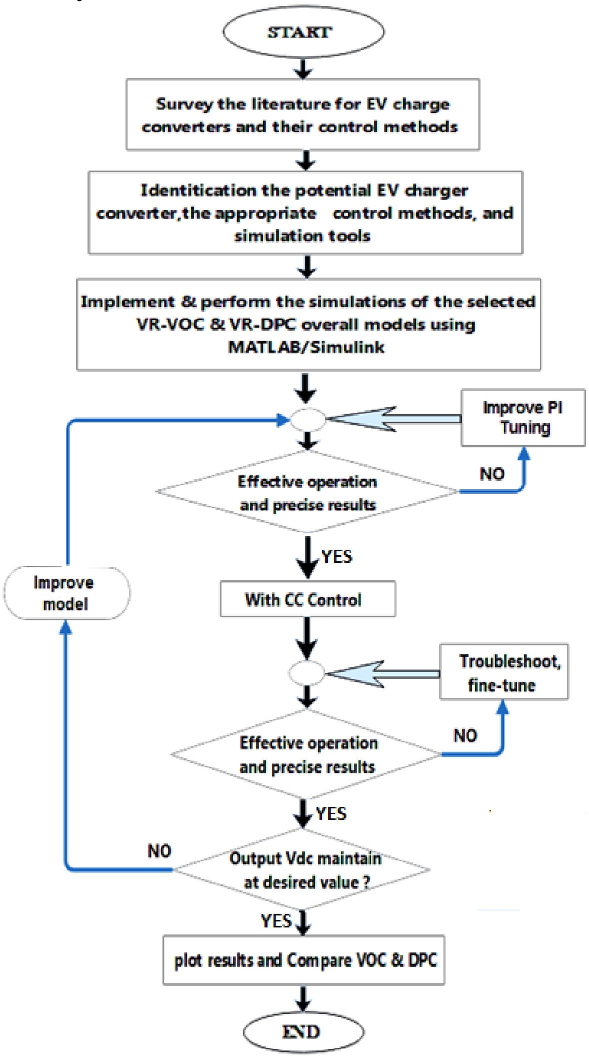

Figure 1. Research methodology flowchart.

- To compare and analyze the obtained results of both VR-VOC and VR-DPC models based on the waveforms of AC input variables, total harmonics distortion of input current, output DC voltage, state of charge of the battery, and the battery voltage.

The rest of this paper will be organized as following, section II deals with the principle operation of Vienna rectifier, more details will be given in section III concerning the VOC and DPC methods, the overall models of VR-VOC and VR-DPC implemented and simulated using Matlab/Simulink software will be the object of section IV, sections V and VI will be dedicated for the results discussion and the conclusions/recommendations respectively.

II. VIENNA RECTIFIER MODELING

The electric circuit representing a 3-ϕ/3-level Vienna rectifier is illustrated in Fig. 2. It consists of six switch devices; each of them is connected anti-parallel with a

diode and stressed by half of the output DC voltage. It is also composed of six diodes, two capacitors at the output DC terminals, and three inductors at the grid side. The neutral point of the three-phase input AC source and that of the output DC-link are grounded. Each phase is represented by a leg with four modes of operation. The three legs have the same behavior with a phase shift of 120° [14]. The current takes different paths depending on the operation mode. The modes for phase-a are formed referring to the variation of source voltage and the state of S_1, S_2, and D_1. The first mode includes the forward bias of D_1 when the source voltage is positive half cycle and transistors are blocked. The current path will be $V_aL_sR_sD_1C_1$. In the second case, the source voltage is still positive half cycle, switches will be forward bias, and diode D_1 is opened. The current takes the path $V_aL_aR_sS_1S_2$. In the third scenario, when the source voltage goes in the negative half cycle and transistors S_1S_2 still conducting. The current follows the way $S_1S_2R_sL_sV_a$. In the last mode of operation, transistors S_1S_2 turned off while the source voltage is still negative half cycle resulting in forward bias D_2. The current flows in the path $C_2D_2R_sL_sV_a$.
Variables S_x (x = a, b, c) are specified as the switching states of the three bidirectional switches to simplify modeling. S_x = 1 or 0 denotes an ON or OFF switch, respectively. The Vienna rectifier's i_o is mathematically determined referring to the circuit configuration, switching states, and the AC source currents as follows [10]:

$$i_0 = S_a i_a + S_b i_b + S_c i_c = - i_{c1} + i_{c2} \qquad (1)$$

The difference between the upper and lower DC-link voltages is referred to as the neutral-point voltage (v_{np}) of the Vienna rectifier. This voltage is impacted by i_o which has the following expression.

$$C\left({}^{dv_{np}}/_{dt}\right) = C\,(d\,(v_{c1} - v_{c2})\,/\,dt) = - i_0 \qquad (2)$$

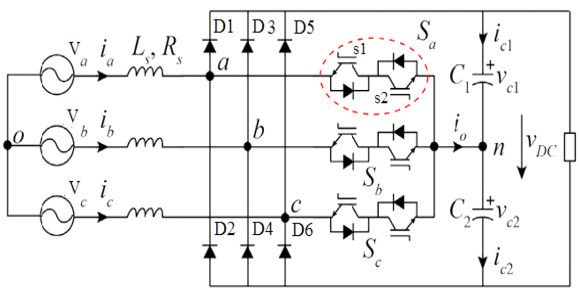

Figure 2. The Circuit model of a three-phase Vienna rectifier.

III. CONTROL STRATEGIES

This section will give a theoretical background related to the selected two control techniques. They are called the voltage-oriented control (VOC) method and the direct power control (DPC) method. The VR will be individually controlled by the VR-VOC and other once by VR-DPC.

A. Voltage-Oriented Control

The VOC approach permits the minimization of interference. With a Hysteresis Pulse Width Modulation (PWM) technology the system performance can be improved [14]. The Phase Locked Loop (PLL) must first be fed with line voltage V_{abc}, and the voltage angle is then utilized to transfer line current and voltage from three phases to dq coordinates. Using the dq coordinate values and the DC link voltage value a decoupled control can be achieved as a second step. Finally, the switching process can be done using the PWM block. S = 1 implies that the upper switch is in conduct mode and lower switch is blocked. If S = 0 indicates that the upper switch is blocked and the lower switch becomes shorted referring to the source voltages [15]. As depicted in Fig. 3, the suggested method uses VOC technology to regulate the charging mechanism with lower current harmonics. Clark and Park transformation matrices are implemented in the two-phases $\alpha\beta 0$ and dq0 domains, where the voltage-oriented controller largely operates [14].

The coordinate transformation is done to create the synchronous rotating coordinate system, which simplifies the system's control structure. The included angle is zero if the d-axis in the d-q coordinate system and the a-axis in the ABC coordinate system are in the same direction. The transformation from ABC to $\alpha\beta$ coordinates is the first stage of the transformation. Secondly, the coordinate $\alpha\beta$ will be transferred to the dq coordinate [16]. By altering the transformation method, the control variables on the AC side become the DC signals. According to the following methods, proportional integral controllers can readily eliminate steady-state errors [1].

$$\begin{bmatrix} v_\alpha \\ v_\beta \end{bmatrix} = \sqrt{\frac{2}{3}} \begin{bmatrix} 1 & \frac{-1}{2} & \frac{-1}{2} \\ 0 & \frac{\sqrt{3}}{2} & -\frac{\sqrt{3}}{2} \end{bmatrix} \begin{bmatrix} v_a \\ v_b \\ v_c \end{bmatrix} \qquad (3)$$

$$\begin{bmatrix} v_d \\ v_q \end{bmatrix} = \begin{bmatrix} \sin\theta & \cos\theta \\ -\cos\theta & \sin\theta \end{bmatrix} \begin{bmatrix} v_\alpha \\ v_\beta \end{bmatrix} \qquad (4)$$

$$V_d^* = K_P(i_{d^*} - i_d) + K_i\,(i_{d^*} - i_d)\,dt \qquad (5)$$

$$V_q^* = K_P\,(i_{q^*} - i_q) + K_i\,(i_{q^*} - i_q)\,dt \qquad (6)$$

K_p and K_i are the gains for the PI controller, i_d and i_q are input currents in the dq0 domain, and i_d^* and i_q^* are the reference signals for i_d and i_q.

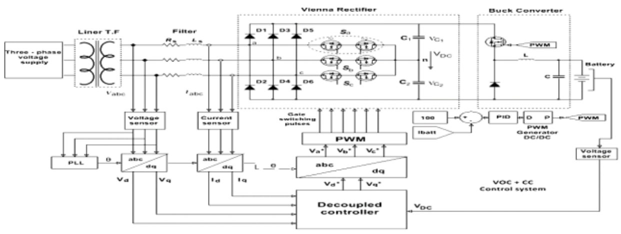
Figure 3. Voltage-oriented control structure for Vienna rectifier.

The operation of the Vienna rectifier has been controlled, as shown in Eq. (7), by using an inverse park transformation after collecting the reference voltages v_d^*

and v_q^* which are utilized to create the gate switching pulses V_{abc}.

$$\begin{bmatrix} v_{\alpha^*} \\ v_{\beta^*} \end{bmatrix} = \begin{bmatrix} \sin\theta & -\cos\theta \\ \cos\theta & \sin\theta \end{bmatrix} \begin{bmatrix} v_{d^*} \\ v_{q^*} \end{bmatrix} \quad (7)$$

B. Direct Power Control

The block diagram of a typical DPC configuration is shown in Fig.4. Zero reactive power q_{ref} and active power p_{ref} reference, which is delivered from the DC bus voltage controller, are compared with the calculated P_s and Q_s values given by Equations (8) and (9), respectively, by means of two-level hysteresis controllers.

$$P_s(t) = v_{sa} . i_{sa} + v_{sb} . i_{sb} + v_{sc} . i_{sc} \quad (8)$$

$$Q_s(t) = \frac{1}{\sqrt{3}} [(v_{sb}\text{-}v_{sc})i_{sa} + (v_{sc}\text{-}v_{sa})i_{sb} + (v_{sa}\text{-}v_{sb})i_{sc} \quad (9)$$

Where; $P_s(t)$ and $Q_s(t)$ are the instantaneous real and imaginary source power.

The control scheme is also based on the cascade control structure, except that the inner loop controller is nonlinear. The DC-link voltage V_{dc} is controlled by a linear PI controller, which provides the reference for the active power P_g^*, whereas the reactive power reference Q_g^* can be set arbitrarily.

IV. PERFORMING SIMULATION

In this section, the implementation of the two studied systems (VR-VOC and VR-DPC) into Matlab/Simulink software will be investigated. The components of each system, input signals, measured signals, output variables, and the corresponding control techniques will be clarified.

A. Vienna Rectifier with VOC

The Matlab/Simulink overall model of VR-VOC is shown in Fig.5. It consists of a three-phase AC inputs system, a three-phase transformer, a three-phase RL lines, the Vienna rectifier, a DC-to-DC buck converter, and a lithium-ion battery as an imposed load to the charging station when the EV plugged-in. More details related to the simulation parameters and the clarification of the adopted control method are given in our previous paper [17].

B. Vienna Rectifier with DPC

The Vienna rectifier is now controlled by a direct power control technique. The Simulink overall model is illustrated in Fig.6. Starting from the measured values of input voltages and currents at the input terminal of the Vienna rectifier, the real active and reactive powers are calculated referring to equations (8) and (9). In this control technique, the reference reactive power is settled to zero value in order to maintain a unity power factor.

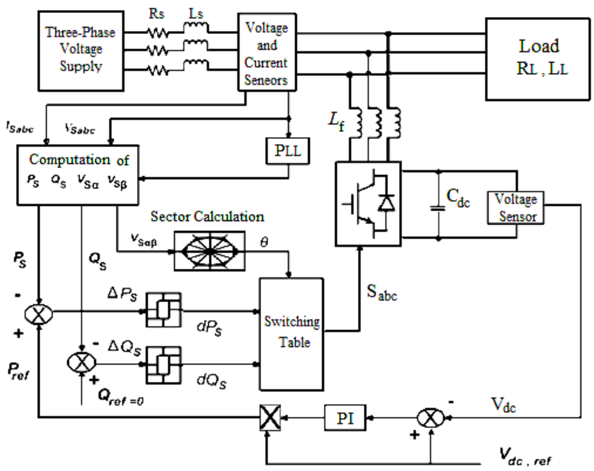

Figure 4. Direct power control structure for Vienna rectifier.

While, the reference active power value is obtained from a proportional integral derivative (PI) controller where the measured value of DC-link voltage is compared with its reference value of 100 V in order to estimate the reference battery charging current. This last is multiplied by the value of DC-link voltage to obtain the reference active power value. The real active and reactive power values are compared with their reference values. The resulting errors from these comparators are entering into limiter blocks then they are used to generate the duty cycle for switching process.

V. RESULTS AND DISCUSSION

In this section, the AC input variables at input terminals of the Vienna rectifier, the output DC-link voltage, the state of charge of the battery, the battery voltage, and the THD of phase-a at 100 A reference constant current will be presented and commented on.

A. AC input variables and output DC voltages

The variation of three-phase voltages applied at the input terminals of the Vienna rectifier due to the use of VOC and DPC techniques are given in Fig.7(a) and Fig.7(b) respectively. They have a sinusoidal variation with respect to the simulation time. Their THDs are kept at very low values due to the closeness in shape to the sin wave. In Fig.8, the injected three-phase currents at the input terminals of the Vienna rectifier for both VOC and DPC methods are illustrated. By using VOC, these currents are slightly affected by the switching procedure, and they have a quasi-sinusoidal shape (Fig.8(a)). When DPC is employed, these currents have more distortion in their shapes due to the switching process (Fig.8(b)). Fig.9 depicts the variation of output DC-link voltage with respect to the simulation time at the output terminals of the Vienna rectifier. It is clearly seen that the adopted control techniques are well operated and fixed the output voltage at more than 90 V DC with a low peak-to-peak ripple voltage using the VOC technique (Fig.9(a)) and at about 100 V DC with high peak-to-peak ripple voltage when DPC technique is employed (Fig9(b)).

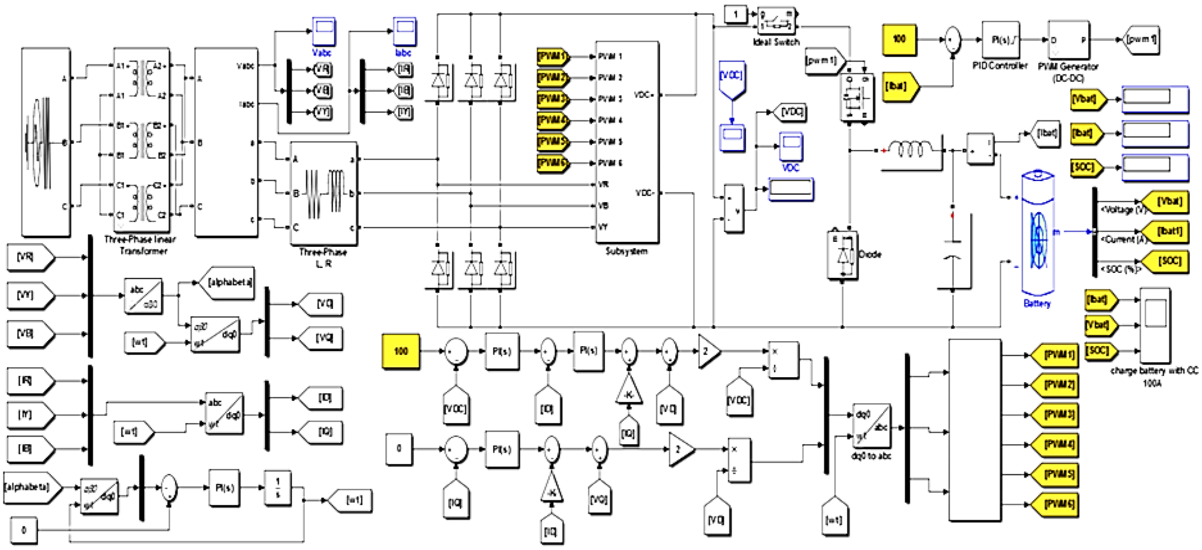

Figure 5. The implemented overall model of VR-VOC.

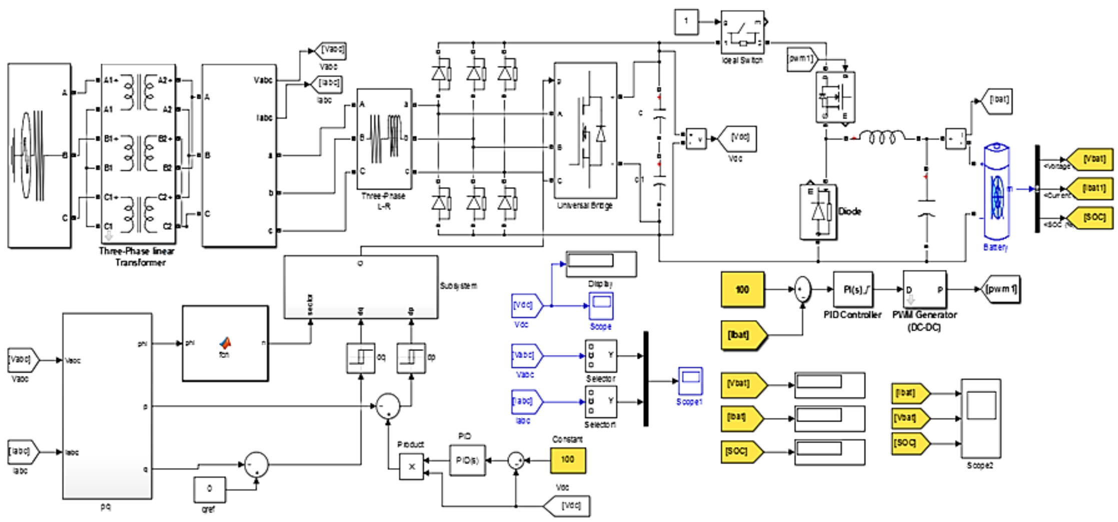

Figure 6. The implemented overall model of VR-DPC.

(a) VR-VOC

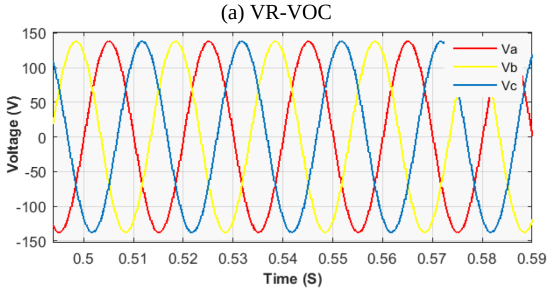

(b) VR-DPC

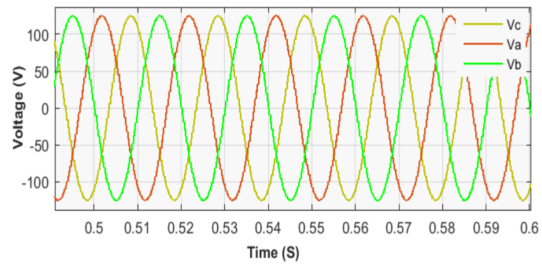

Figure 7. The three-phase voltage variations.

(a) VR-VOC

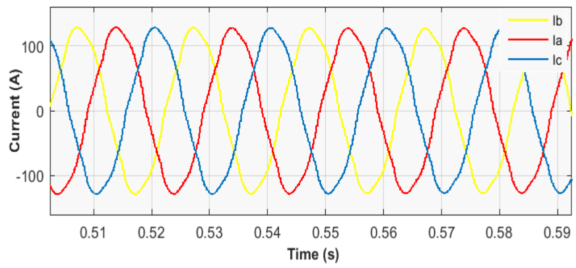

(b) VR-DPC

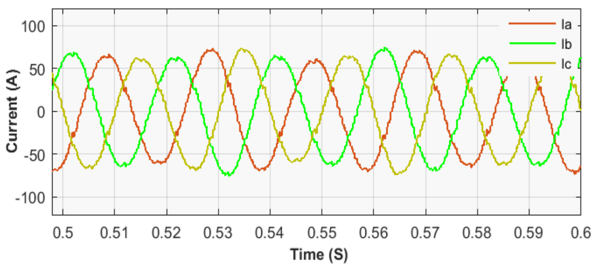

Figure 8. The three-phase current variations.

(a) VR-VOC

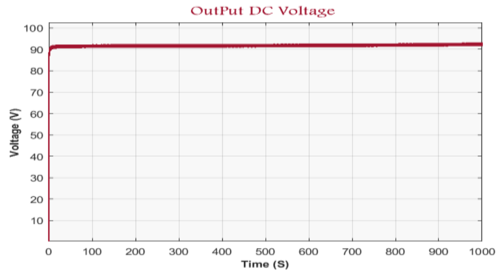

(b) VR-DPC

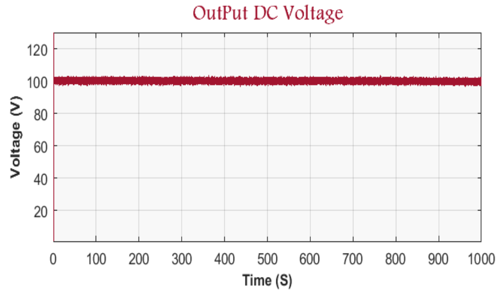

Figure 9. The output DC-link voltages

B. *SoC and voltage of the battery*

Starting from an initial value of 80 % state of charge of the battery and at different charging constant current values of (60A, 80A, and 100A) for both VOC and DPC, the SoC is shown in Fig.10(a) and Fig.10(b) respectively. By using VOC or DPC control method, the obtained SoCs have the same shape. It can be seen that the higher the battery charging current the faster the battery full-charge. The battery reaches its full-charge at about 860 seconds when charging current of 100 A is injected into the battery, while more than 1000 seconds is needed to reach the full-charge when 80 A or 60 A is applied. Fig.11 illustrates the variation of battery voltage with respect to the simulation time at different constant currents of 60, 80, and 100 A for both VOC and DPC methods. The same behavior is also obtained for the both control techniques. When a charging current of 100 A is imposed, the battery voltage has a constant value of about 53 volts from origin point until 500 seconds that is corresponding to more than 90 % SoC. After this, an increase of about 6 Volts is gained until the full-charge at 860 seconds. A slight increase of one volt with linear behavior is observed from full-charge instant until the end of simulation time. The same behavior is occurred at 80 A and 60 A but with a wider range of charging time.

C. *THD of phase-a of input current at CC of 100A*

Fig.12 depicts the THD of input current at the input terminals of the Vienna rectifier when charging constant current of 100 A is imposed to charge the EV battery for both VOC and DPC methods. The content of harmonics injected into the grid due to the switching process of the converter using VOC is at low value of 1.87 % because of the quasi-sine wave of current. A high harmonic contents of 5.88 % injected into the main line, at which the VR is connected, can be observed as a result of the distortion of the current waveform when DPC technique is adopted.

(a) VR-VOC

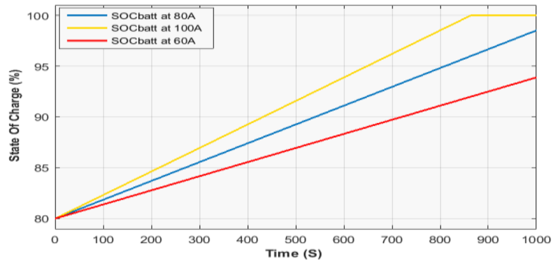

(b) VR-DPC

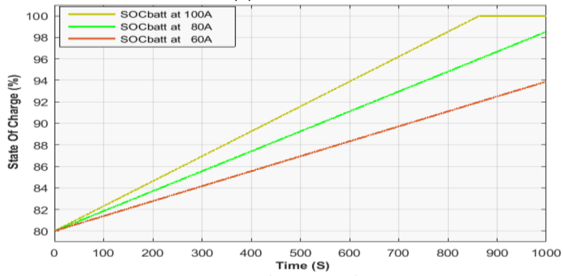

Figure 10. State of charge of the battery.

(a) VR-VOC

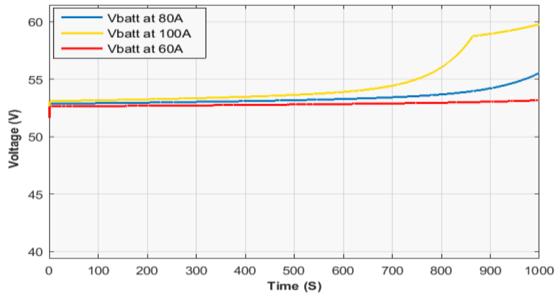

(b) VR-DPC

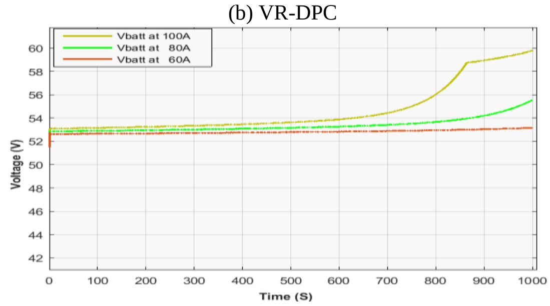

Figure 11. Battery voltage.

VI. CONCLUSIONS AND RECOMMENDATIONS

This work is dealt with the comparing of two control methods namely VOC and DPC in order to control an off-board Vienna rectifier for charging an EV battery from a national grid using the software Matlab/Simulink. The conclusions that can be drawn are as follows:

- The three-phase input voltages imposed at the input terminals of the VR are slightly affected by the switching process. They almost have the same sine waveforms for both VOC and DPC methods.
- The drawn three-phase currents from the grid have quasi-sine waves when VOC technique is used resulting in a low THD of 1.87 %. While, when DPC technique is employed, they contained more harmonics with a high THD of 5.88%.

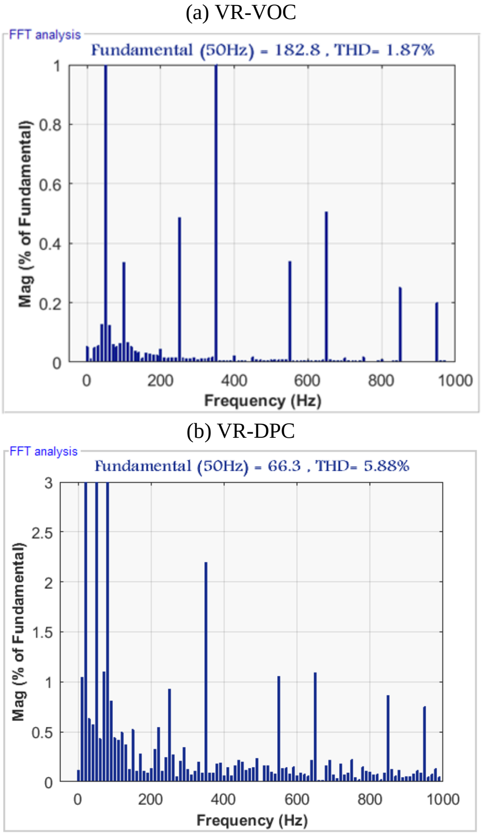

Figure 12. THD of current of phase-a for charging current of 100 A.

- The SoC of the battery and its voltage level are not affected by the control techniques. For both VOC and DPC, they have the same variations.
- The VOC method has superiority over the DPC method in terms of the sine-wave closeness and the THD but in terms of simulation time; it takes more time comparing the DPC.

In terms of recommendations, many tasks may have been added to the present research in order to improve its contribution. Firstly, an experiment can be realized, and then compare the obtained results with those obtained by the simulation presented in this work. Secondly, introducing the artificial intelligence to optimize the switching process. Finally, an economic study can be reflecting the benefits of the transition to electric vehicle adoption.

REFERENCES

[1] L. Bao, L. Fan and Z. Miao, "Real-Time Simulation of Electric Vehicle Battery Charging Systems," 2018 North American Power Symposium (NAPS), Fargo, ND, USA, 2018, pp. 1-6, doi: 10.1109/NAPS.2018.8600543.

[2] M. Safayatullah, M. T. Elrais, S. Ghosh, R. Rezaii and I. Batarseh, "A Comprehensive Review of Power Converter Topologies and Control Methods for Electric Vehicle Fast Charging Applications," in IEEE Access, vol. 10, pp. 40753-40793, 2022, doi: 10.1109/ACCESS.2022.3166935.

[3] Al-Ogaili AS, Aris IB, Verayiah R, Ramasamy A, Marsadek M, Rahmat NA, Hoon Y, Aljanad A, Al-Masri AN. A Three-Level Universal Electric Vehicle Charger Based on Voltage-Oriented Control and Pulse-Width Modulation. *Energies*. 2019; 12(12):2375. https://doi.org/10.3390/en12122375

[4] Arif SM, Lie TT, Seet BC, Ayyadi S, Jensen K. Review of Electric Vehicle Technologies, Charging Methods, Standards and Optimization Techniques. *Electronics*. 2021; 10(16):1910. https://doi.org/10.3390/electronics10161910

[5] Jaman S, Chakraborty S, Tran D-D, Geury T, El Baghdadi M, Hegazy O. Review on Integrated On-Board Charger-Traction Systems: V2G Topologies, Control Approaches, Standards and Power Density State-of-the-Art for Electric Vehicle. *Energies*. 2022; 15(15):5376. https://doi.org/10.3390/en15155376

[6] Valedsaravi S, El Aroudi A, Martínez-Salamero L. Review of Solid-State Transformer Applications on Electric Vehicle DC Ultra-Fast Charging Station. *Energies*. 2022; 15(15):5602. https://doi.org/10.3390/en15155602

[7] Polat H, Hosseinabadi F, Hasan MM, Chakraborty S, Geury T, El Baghdadi M, Wilkins S, Hegazy O. A Review of DC Fast Chargers with BESS for Electric Vehicles: Topology, Battery, Reliability Oriented Control and Cooling Perspectives. *Batteries*. 2023; 9(2):121. https://doi.org/10.3390/batteries9020121

[8] Kumar Nishant, K. Prabha Rani, K. V. S. R. Murthy. Comparative Analysis of Different Topologies of Vienna Rectifier. IOS Press, Volume 27: Advanced Production and Industrial Engineering, 2022.pp. 163 – 168, doi: 10.3233/ATDE220736

[9] Y. Wang, Y. Li and S. Huang, "An Improved Sliding Mode Direct Power Control Strategy Based on Reactive Power Compensation for Vienna Rectifier," in IEEE Access, vol. 10, pp. 15469-15477, 2022, doi: 10.1109/ACCESS.2022.3149042.

[10] G. Rajendran, C. A. Vaithilingam, N. Misron, K. Naidu and M. R. Ahmed, "Voltage Oriented Controller Based Vienna Rectifier for Electric Vehicle Charging Stations," in IEEE Access, vol. 9, pp. 50798-50809, 2021, doi: 10.1109/ACCESS.2021.3068653.

[11] J. -C. Kim and S. Kwak, "Direct Power Control Method with Minimum Reactive Power Reference for Three-Phase AC-to-DC Matrix Rectifiers Using Space Vector Modulation," in IEEE Access, vol. 7, pp. 67515-67525, 2019, doi: 10.1109/ACCESS.2019.2918571.

[12] Lan Chen, Huihui Xiao, Qiang Guo, Shuxi Liu, Chaojun Sun (2020). Direct Power Control Strategy for Three-phase Vienna Rectifier. Journal of Physics: Conference Series, Volume 1754, 2020 3rd International Symposium on Power Electronics and Control Engineering (ISPECE 2020) 27-29 November 2020. DOI 10.1088/1742-6596/1754/1/012115

[13] Hui Ma, Yunxiang Xie, Biaoguang Sun, Lingjun Mo (2015). Modeling and Direct Power Control Method of Vienna Rectifiers Using the Sliding Mode Control Approach. Journal of Power Electronics, Vol. 15, No. 1, pp. 190-201, January 2015, doi: 10.6113/JPE.2015.15.1.190

[14] B. Xu, K. Liu, X. Ran, and Q. Huai, "Model predictive duty cycle control for three-phase Vienna rectifiers," IET Power Electronics, vol. 15, pp. 447-461, 2022. doi:10.1049/pel2.12244

[15] Hoon Y, Mohd Radzi MA, Hassan MK, Mailah NF. DC-Link Capacitor Voltage Regulation for Three-Phase Three-Level Inverter-Based Shunt Active Power Filter with Inverted Error Deviation Control. *Energies*. 2016; 9(7):533. https://doi.org/10.3390/en9070533

[16] F. Dai, Y. Zhu, D. Yin, and Y. Yuan, "Research of the Control Strategy of VIENNA Rectifier Circuit based on the Vector Control," Journal of Robotics, Networking and Artificial Life, vol. 7, pp. 12-15, 2020. doi:10.2991/jrnal.k.200512.003

[17] W. S. Ali, A. Nouh, M. A. Faraj and F. Mohamed, "Adoption of Vienna Rectifier with Voltage-Oriented Control Technique based Electric Vehicles Charging Stations for Future Integration into a Local Network," 2022 13th International Renewable Energy Congress (IREC), Hammamet, Tunisia, 2022, pp. 1-6, doi: 10.1109/IREC56325.2022.10001951